

The radio luminosity, black hole mass and Eddington ratio for quasars from the Sloan Digital Sky Survey

Wei-Hao. Bian^{1,2}, Yan-Mei. Chen¹, Chen. Hu³, kai. Huang² and Yan. Xu²

¹ Key Laboratory for Particle Astrophysics, Institute of High Energy Physics, Chinese Academy of Sciences, Beijing 100039, China

² Department of Physics and Institute of Theoretical Physics, Nanjing Normal University, Nanjing 210097, China

³ National Astronomical Observatories, Chinese Academy of Sciences, Beijing 100012, China

Abstract We investigate the $M_{\text{BH}} - \sigma_*$ relation for radio-loud quasars with redshift $z < 0.83$ in Data Release 3 of the Sloan Digital Sky Survey (SDSS). The sample consists of 3772 quasars with better model of $\text{H}\beta$ and $[\text{O III}]$ lines and available radio luminosity, including 306 radio-loud quasars, 3466 radio-quiet quasars with measured radio luminosity or upper-limit of radio luminosity (181 radio-quiet quasars with measured radio luminosity). The virial supermassive black hole mass (M_{BH}) is calculated from the broad $\text{H}\beta$ line, the host stellar velocity dispersion (σ_*) is traced by the core $[\text{O III}]$ gaseous velocity dispersion, and the radio luminosity and the radio loudness are derived from the FIRST catalog. Our results are follows: (1) For radio-quiet quasars, we confirm that there is no obvious deviation from the $M_{\text{BH}} - \sigma_*$ relation defined in inactive galaxies when M_{BH} uncertainties and luminosity bias are concerned. (2) We find that radio-loud quasars deviate much from the $M_{\text{BH}} - \sigma_*$ relation respect to that for radio-quiet quasars. This deviation is only partly due to the possible cosmology evolution of the $M_{\text{BH}} - \sigma_*$ relation and the luminosity bias. (3) The radio luminosity is proportional to $M_{\text{BH}}^{1.28^{+0.23}_{-0.16}} (L_{\text{Bol}}/L_{\text{Edd}})^{1.29^{+0.31}_{-0.24}}$ for radio-quiet quasars and $M_{\text{BH}}^{3.10^{+0.60}_{-0.70}} (L_{\text{Bol}}/L_{\text{Edd}})^{4.18^{+1.40}_{-1.10}}$ for radio-loud quasars. The weaker correlation of the radio luminosity dependence upon the mass and the Eddington ratio for radio-loud quasars shows that other physical effects would account for their radio luminosities, such as the black hole spin.

Key words: quasars: emission lines — galaxies: nuclei — galaxies: bulges — black hole physics

1 INTRODUCTION

The relation between the supermassive black hole (SMBH) mass and the host stellar velocity dispersion (hereafter $M_{\text{BH}} - \sigma_*$ relation) is one of the most important results in the study of supermassive black holes (SMBHs) in these decades, implying the intimate correlation between the SMBHs and their host galaxies (e.g. Gebhardt et al. 2000; Ferrarese & Merrit 2000; Tremaine et al. 2002; Lauer et al. 2007). This correlation would provide strong constraints for the evolution of active galactic nuclei (AGNs) if we know

* Supported by the National Natural Science Foundation of China.

* E-mail: bianwh@ihep.ac.cn

AGNs follow this relation or not. However it is still under debate for different kind of AGNs, such as radio-loud AGNs, narrow-line Seyfert 1 galaxies, intermediate supermassive black hole, et al. (e.g., Nelson 2001; Boroson 2003; Shield et al. 2003; Bian & Zhao 2004; Grupe & Mathur 2004; Bonning et al. 2005; Greene & Ho 2006; Woo et al. 2006; Zhou et al. 2006; Salviander et al. 2007; Komossa & Xu 2007; Shen et al. 2008). In order to study this relation for AGNs, we should calculate M_{BH} and σ_* as accurately as possible.

The width of the broad emission line (e.g., $\text{H}\beta$, $\text{H}\alpha$, Mg II , C IV) can be used to trace virial velocity of the clouds in broad line regions (BLRs) when the line contribution from narrow-line regions (NLRs) is reasonably removed, and the reverberation mapping method or the empirical luminosity-size relation can be used to calculate the BLRs size (e.g., Kaspi et al. 2000; McLure & Dunlop 2004; Bian & Zhao 2004; Peterson et al., 2004; Greene & Ho 2005b). The gas velocity dispersion of the narrow lines (e.g., $[\text{O III}]$, $[\text{O II}]$, $[\text{S II}]$) from NLRs are usually used to trace the host stellar velocity dispersion (e.g., Nelson & Whittle 1996; Greene & Ho 2005a). We also can directly measure the host velocity dispersion from AGNs host spectra (e.g., Kauffmann et al. 2003; Heckman et al. 2004; Greene & Ho 2005a; Bian et al. 2006). The larger number of quasars found in the Sloan Digital Sky Survey (SDSS) provides the possibility to tackle the $M_{\text{BH}} - \sigma_*$ relation in radio-loud quasars. (e.g. Bian & Zhao 2004; Salviander et al. 2007).

The dichotomy of the radio loudness in quasars is a long-time question since the discovery of quasars (Sandage 1965; Strittmatter et al. 1980; Kellermann et al. 1989). The radio luminosity is assumed coming from the relativistic electrons powered by a jet, which is intimately connected with the SMBH (e.g., Begelman et al. 1984; Blundell & Beasley 1998). For scale-free jet physics and accretion theories, the radio luminosity is related to the central engines, such the SMBH mass, the SMBH spin, the Eddington ratio, et al. (Heinz & Sunyaev 2003). For radio-loud or radio-quiet quasars, the dependence of the radio loudness/luminosity upon the SMBH mass/Eddington ratio is discussed by many peoples, some support it and some against it. (e.g., Franceschini et al. 1998; Laor 2000; Lacy et al. 2001; Ho 2002; Woo & Urry 2002; McLure & Jarvis 2004; Wang et al. 2004; Greene et al. 2006; Liu et al. 2006; Sikora 2007; Panessa et al. 2007). Laor (2003) gave some comments on the origin of AGNs radio loudness and discussed the some error SMBH mass estimation for radio-loud AGNs in the literature, which is mainly due to optical spectra with low signal-to-noise ratios, no correction of $\text{H}\beta$ contribution from narrow line regions (NLRs).

In this paper, we use larger number of quasars with redshifts $z < 0.83$ in SDSS Data Release 3 (DR3; see Abazajian et al. 2005) to investigate the $M_{\text{BH}} - \sigma_*$ relation and the radio luminosity dependence on the SMBH mass and the Eddington ratio for radio-loud and radio-quiet quasars. In §2, we briefly introduce the SDSS quasars Data Release 3 catalog of Schneider et al. (2005). §3 is the data analysis. §4 introduces the methods to calculate the SMBH masses and the Eddington ratios. Our results and discussions of $M_{\text{BH}} - \sigma_*$ relation and the origin of radio luminosity are given in §5 and §6, respectively. The last section is our conclusions. All of the cosmological calculations in this paper assume $H_0 = 70 \text{ km s}^{-1} \text{ Mpc}^{-1}$, $\Omega_{\text{M}} = 0.3$, $\Omega_{\Lambda} = 0.7$.

2 SAMPLE AND DATA ANALYSIS

The sample used in this paper is selected from the SDSS quasars Catalog III, which covers a spectroscopic area of 1360 sq. deg., about 40% of the proposed SDSS survey area (Schneider et al. 2003). This catalog consists of 46,420 quasars in SDSS DR3 with $M_i < -22$. The catalog also contains radio emission properties from Faint Images of the Radio Sky at Twenty-cm (FIRST) survey within 2.0" of the quasars position (see Col. 17 in their Table 1).

SDSS optical spectra cover the wavelength range 3800-9200 Å with a resolution of $1800 < R < 2100$. In order to calculate SMBH mass from the broad $\text{H}\beta$ line and the host stellar velocity dispersion from the narrow $[\text{O III}]$ line, we just consider the quasars with redshifts less than 0.83, which consists of 9753 quasars. Because whether the SMBH mass from Mg II linewidth is consistent with that from $\text{H}\beta$ line width is still a complex question (e.g., Salviander et al. 2007), here we don't consider using Mg II linewidth to calculate the SMBH mass.

The radio luminosity at 5GHz is calculated from the peak flux density listed in Col. 17 in Table 2 (Schneider et al. 2003), considering the spectral index of $\alpha = 0.5$, where $f_{\nu} \propto \nu^{-\alpha}$. The radio loudness R is calculated from: $R = f_{5\text{GHz}}/f_{\text{B}}$, where $f_{5\text{GHz}}$ and f_{B} are the rest-frame flux density at 5 GHz and

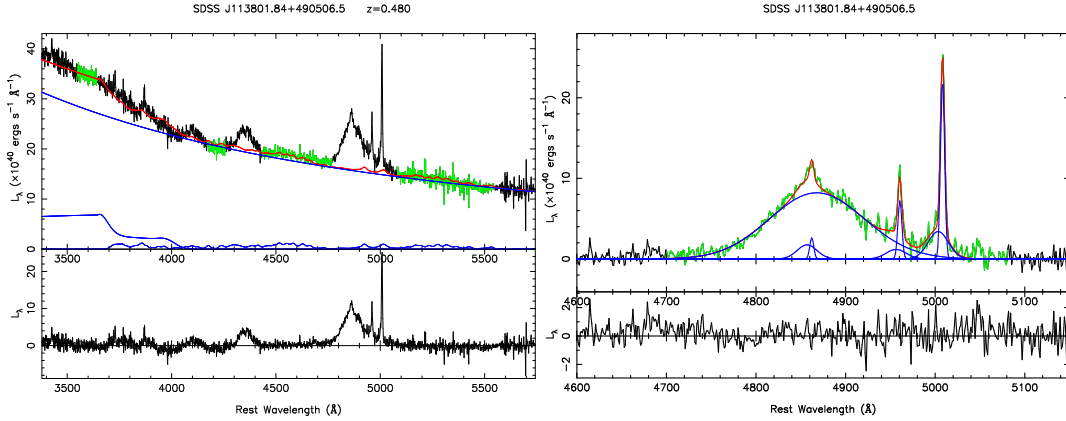


Fig. 1 Sample of SDSS spectrum measurement for SDSS J113801.84+490506.5. In the top panel, the black curve is the observed spectrum, the red line is the sum of the power-law continuum, the Balmer continuum and Fe II multiples (blue curves). The green ranges are our fitting windows. The bottom panel is the multi-Gaussian fit for $H\beta$ and [O III] lines. The red line is the sum of all multi-Gaussian (blue curves). The green curve is our fitting range of the pure $H\beta$ and [O III] emissions after the subtraction of the power-law continuum, the Balmer continuum and Fe II multiples.

4400Å, considering k correction. $R = 10$ is commonly used to define radio-loud quasars and radio-quiet quasars (e.g., McLure & Jarvis 2004), as well as the radio luminosity at 5 GHz (e.g., Lacy 2001).

For 9573 quasars with $z < 0.83$ from SDSS DR3, 914 quasars are detected by FIRST, 7846 quasars are under the FIRST flux limit, and 993 quasars are not in the region covered by FIRST. For these objects with non-detection in FIRST, we only have the upper-limits of the radio luminosity and the radio loudness. 598 quasars with detection in FIRST and $R \geq 10$ are classified as radio-loud quasars. 316 quasars with detection in FIRST and $R < 10$ are classified as radio-quiet quasars. 5712 quasars with non-detection in FIRST and $R < 10$ are classified as radio-quiet quasars but with upper-limits of R and the radio luminosity.

As we know, NLRs can contribute $H\beta$ emission in the total $H\beta$ profile; [O III] usually shows non-symmetric profile and its narrow/core component can trace the stellar velocity better (e.g., Greene & Ho 2005a); optical and ultraviolet Fe II multiples are often presented in quasars spectra; Balmer continuum is required because of the existence of strong Balmer emission lines, therefore, we use following steps to do the SDSS spectral measurements.

(1) First, we do the Galactic extinction in the observed spectra by using the extinction law of Cardelli, Clayton & Mathis (1989) (IR band) and O'Donnell (1994) (optical band), then the spectra are transformed into the rest frame defined by the redshifts given in their FITS headers.

(2) The optical and ultraviolet Fe II template from the prototype NLS1 I ZW 1 is used to subtract the Fe II emission from the spectra (Boroson & Green 1992; Vestergaard & Wilkes 2001). The I ZW 1 template is broadened by convolving with a Gaussian of various linewidths and scaled by multiplying a factor. A power-law continuum and the Balmer continuum are added in the fitting. We calculate the Balmer continuum following Grandi (1982) and also add the high order Balmer lines at the red side of the Balmer edge using the result in Storey & Hummer(1995). The best subtraction of the Fe II, power-law and Balmer continuum is found when χ^2 minimized in the fitting windows: 3550-3645, 4170-4260, 4430-4770, 5080-5550, 6050-6200, 6890-7010Å (see a sample fit in the top panel of Figure 1). The monochromatic luminosity at 5100Å ($\lambda L_\lambda(5100\text{Å})$) is calculate from the power-law continuum.

(3) Two sets of two-Gaussian are used to model [O III] $\lambda\lambda 4959, 5007$ lines. Three-Gaussian is used to model $H\beta$ line. For the doublet [O III] $\lambda\lambda 4959, 5007$, we take the same linewidth for each component, and fix the flux ratio of [O III] $\lambda 4959$ to [O III] $\lambda 5007$ to be 1:3. Two components of $H\beta$ (supposed from NLRs) are set to have the same linewidth of each component of [O III] $\lambda 5007$ and their flux are constrained to be

less than 1/2 of each component of [O III] $\lambda 5007$. The linewidth of the broad component of $H\beta$ is used to trace the virial velocity around central SMBH (see a sample fit in the bottom panel of Figure 1).

From above spectral measurement, we obtain the full width at half maximum (FWHM) of the broad $H\beta$ line and the narrow/core [O III] line ($\text{FWHM}_{H\beta}$, $\text{FWHM}_{[\text{OIII}]}$), the monochromatic luminosity at 5100\AA ($\lambda L_{\lambda}(5100\text{\AA})$), the total $H\beta$ luminosity ($L_{H\beta}$), as well as the radio luminosity and the radio loudness for SDSS DR3 quasars with $z < 0.83$.

Objects without the $H\beta$ or [O III] lines are eliminated. In order to obtain the reliable spectra fit, we carefully select objects for analysis. The line equivalent width (EW) can show line signal-to-noise ratios. The error of EW can be regarded as a tracer to show the fitting goodness. Because the $H\beta$ is usually strong, we don't constrain EW of $H\beta$ line, only constrain the error of EW for $H\beta$ line. We select objects by the criterions of EW of [O III] larger than 1.5, the errors of EWs of $H\beta$ and [O III] $\lambda\lambda 4959, 5007$ less than 100%. It leads to 367 radio-loud quasars, 3677 radio-quiet quasars including 207 radio-quiet quasars with measured radio luminosity. Then we visually check these spectra one by one.

At last, we obtain a sample of 3772 quasars with better multi-components model of $H\beta$ and [O III] lines, including 3466 radio-quiet quasars (hereafter "RQ total sample"), 306 radio-loud quasars (hereafter "RL sample"). Most objects in these 3466 radio-quiet quasars only have upper-limits of the radio luminosity and the radio loudness, 181 radio-quiet quasars (hereafter "RQ sample") have the measurements of the radio luminosity and the radio loudness. We use the radio-quiet sample as the control sample to discuss the $M_{\text{BH}} - \sigma_*$ in radio-loud quasars.

3 SMBH MASS, EDDINGTON RATIO AND STELLAR VELOCITY DISPERSION

The BLRs size is calculated from the monochromatic luminosity at 5100\AA ($\lambda L_{\lambda}(5100\text{\AA})$) or the $H\beta$ luminosity by the following formulae (Kaspi et al. 2005):

$$R_{\text{BLR}}^{\lambda L_{\lambda}(5100\text{\AA})} = (22.3 \pm 2.1) \left(\frac{\lambda L_{\lambda}(5100\text{\AA})}{10^{44} \text{ erg s}^{-1}} \right)^{0.69 \pm 0.05} \text{ lt - days} \quad (1)$$

$$R_{\text{BLR}}^{L_{H\beta}} = (82.3 \pm 7.0) \left(\frac{L_{H\beta}}{10^{43} \text{ erg s}^{-1}} \right)^{0.80 \pm 0.11} \text{ lt - days} \quad (2)$$

We use the FWHM of the broad $H\beta$ line ($\text{FWHM}_{H\beta}$) to trace the BLRs virial velocity $v_{\text{BLR}} = \sqrt{f} \times \text{FWHM}_{H\beta}$, f is the calibration factor. If BLRs cloud is disk-like with a inclination of θ (Wills & Browne 1986),

$$\text{FWHM}_{H\beta} = 2(v_r^2 + v_{\text{BLR}}^2 \sin^2 \theta)^{1/2} \quad (3)$$

where v_r is the random isotropic component. We can then calculate the SMBH masses by $M_{\text{BH}} = \frac{R_{\text{BLR}} v_{\text{BLR}}^2}{G}$ (Kaspi et al. 2000; Kaspi et al. 2005):

$$M_{\text{BH}} = f \times 4.35 \times 10^6 \left(\frac{\text{FWHM}_{H\beta}}{10^3 \text{ km s}^{-1}} \right)^2 \left(\frac{\lambda L_{\lambda}(5100\text{\AA})}{10^{44} \text{ erg s}^{-1}} \right)^{0.69} M_{\odot}. \quad (4)$$

$$M_{\text{BH}} = f \times 1.61 \times 10^7 \left(\frac{\text{FWHM}_{H\beta}}{10^3 \text{ km s}^{-1}} \right)^2 \left(\frac{L_{H\beta}}{10^{43} \text{ erg s}^{-1}} \right)^{0.80} M_{\odot}. \quad (5)$$

If assuming $v_r \ll v_{\text{BLR}}$, and the random orbits of BLRs clouds, $f = 0.75$. Onken et al. (2004) did a calibration by the $M_{\text{BH}} - \sigma_*$ relation and suggested $f \approx 1.4$ (see also Collin et al. 2006; Dasyra et al. 2007). In our mass calculation, we adopt the random orbits of BLRs clouds and $f = 0.75$.

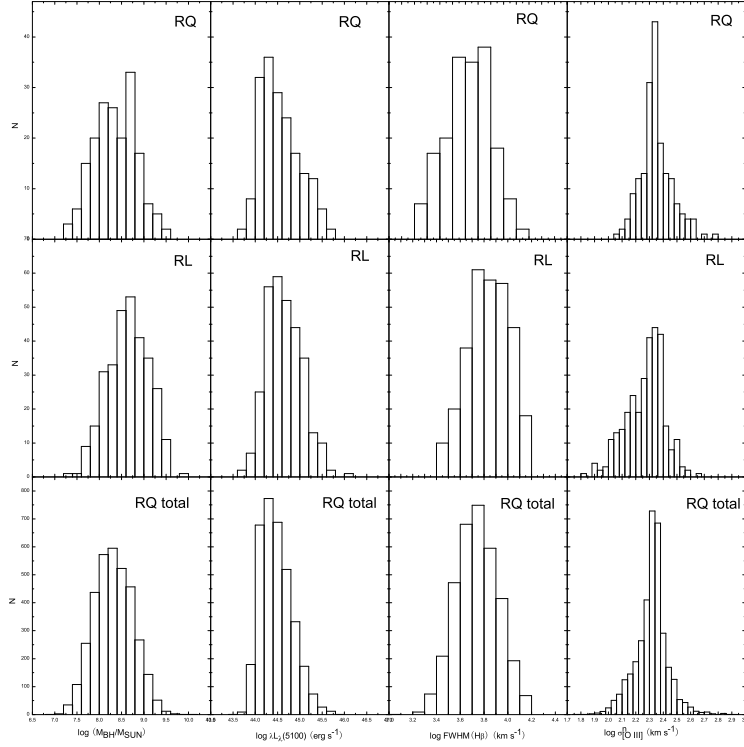


Fig. 2 The distributions of M_{BH} , $\lambda L_{\lambda}(5100\text{\AA})$, $\text{FWHM}_{\text{H}\beta}$, $\sigma_{[\text{O III}]}$ for 181 radio-quiet quasars with radio loudness (top), 306 radio-loud quasars with measured radio luminosity (middle), total 3466 radio-quiet quasars (bottom).

We calculate the Eddington ratio, i.e., the ratio of the bolometric luminosity (L_{bol}) to the Eddington luminosity (L_{Edd}), where $L_{\text{Edd}} = 1.26 \times 10^{38} (M_{\text{BH}}/M_{\odot}) \text{erg s}^{-1}$. The bolometric luminosity is calculated from the monochromatic luminosity at 5100\AA , $L_{\text{bol}} = c_{\text{B}} \lambda L_{\lambda}(5100\text{\AA})$, where we adopt the correction factor c_{B} of 9 (Kaspi et al. 2000; Marconi et al. 2004; Richards et al. 2006; Netzer & Trakhtenbrot 2007).

We use the gas velocity dispersion of the narrow/core [O III] component from NLRs to trace the host stellar velocity dispersion, $\sigma_{[\text{O III}]}^n = \sqrt{\sigma_{\text{obs}}^2 - [\sigma_{\text{inst}}/(1+z)]^2}$, where $\sigma_{\text{obs}} = \text{FWHM}_{[\text{O III}]}^n/2.35$, z is the redshift (Bian et al. 2006). For SDSS spectra, the mean value of instrument resolution σ_{inst} is 60 km s^{-1} for [O III] (e.g. Greene & Ho 2005a).

In Figure 2, we present the distributions of the SMBH mass, $\lambda L_{\lambda}(5100\text{\AA})$, $\text{FWHM}_{\text{H}\beta}$, $\sigma_{[\text{O III}]}$ for 181 radio-quiet quasars with radio loudness (top), 306 radio-loud quasars with measured radio luminosity (middle), total 3466 radio-quiet quasars (bottom). The mean of SMBH mass is 8.65 ± 0.03 with a standard deviation of 0.45 for RL sample of 306 radio-loud quasars, 8.36 ± 0.04 with a standard deviation of 0.48 for RQ sample of 181 radio-quiet quasars with reliable radio luminosity, 8.32 ± 0.01 with a standard deviation of 0.43 for total 3466 radio-quiet quasars. Radio-loud quasars have larger SMBH masses, and there is only a few objects with mass less than $10^8 M_{\odot}$ (see Figure 3), which is consistent with the results of McLure & Jarvis (2004). Radio-loud quasars have smaller Eddington ratios, respect to radio-quiet quasars (see Table 1). We find that, for radio-loud quasars, the mean of $\text{H}\beta$ FWHM is $7493 \pm 165 \text{ km s}^{-1}$ with a standard deviation of 2882 km s^{-1} , the mean of $\log \lambda L_{\lambda}(5100\text{\AA})$ is $44.86 \pm 0.03 \text{ erg s}^{-1}$ with a standard deviation of 0.45; for radio-quiet quasars, the mean of $\text{H}\beta$ FWHM is $5780 \pm 176 \text{ km s}^{-1}$ with a standard deviation

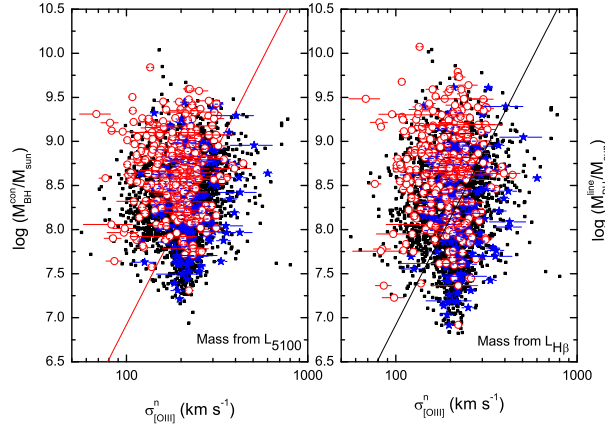


Fig. 3 The $M_{\text{BH}} - \sigma_*$ relation for radio-loud and radio-quiet quasars. Red circle denotes radio-loud quasars, blue star denotes radio-quiet quasars with measured radio luminosity, black square denotes the radio-quiet quasars with upper-limit of the radio luminosity. The mass in the left panel is derived from $\lambda L_{\lambda}(5100\text{\AA})$, and the mass in the right panel is derived from $H\beta$ luminosity.

of 2389 km s^{-1} , the mean of $\log \lambda L_{\lambda}(5100\text{\AA})$ is $44.81 \pm 0.01 \text{ erg s}^{-1}$ with a standard deviation of 0.46. Radio-loud quasars tend to have larger $H\beta$ FWHM and $\lambda L_{\lambda}(5100\text{\AA})$, leading larger SMBH masses (Sulentic et al. 2000).

4 $M_{\text{BH}} - \sigma_*$ RELATION

4.1 The mass deviation from $M_{\text{BH}} - \sigma_*$ relation

In Figure 3, we show $M_{\text{BH}} - \sigma_*$ relation for radio-loud and radio-quiet quasars. The solid line in Figure 3 is the $M_{\text{BH}} - \sigma_*$ relation in normal nearby galaxies given by Tremaine et al. (2002), $M_{\text{BH}}(\sigma_*) = 10^{8.13} [\sigma_*/(200 \text{ km s}^{-1})]^{4.02} M_{\odot}$. In the left and right panels of Figure 3, $\lambda L_{\lambda}(5100\text{\AA})$ and $L_{H\beta}$ are used to calculate the SMBH mass, respectively. In Figure 3, the correlation between M_{BH} and $\sigma_{[\text{O III}]}$ is very weak for larger SDSS quasars sample. It is possibly due to the accuracy of the stellar velocity dispersion derived from the narrow/core [O III] line-width. However, it is obvious that the sample of radio-loud quasars deviated much from the solid line respect to that for the sample of radio-quiet quasars. It is consistent with our previous result (Bian & Zhao 2004).

We calculate the black hole mass deviation $\Delta \log M_{\text{BH}}$ from the solid line defined by Tremaine et al. (2002), $\Delta \log M_{\text{BH}} = \log M_{\text{BH}}(H\beta) - \log M_{\text{BH}}(\sigma_*)$, where σ_* is adopted to be $\sigma_{[\text{O III}]}$. For the mass derived from $\lambda L_{\lambda}(5100\text{\AA})$, the mean of $\Delta \log M_{\text{BH}}$ is 0.65 ± 0.04 with a standard deviation of 0.71 for RL sample of 306 radio-loud quasars, 0.04 ± 0.04 with a standard deviation of 0.63 for RQ sample of 181 radio-quiet quasars with reliable radio luminosity, 0.14 ± 0.01 with a standard deviation of 0.62 for total 3466 radio-quiet quasars. We find that they are almost the same for the case of the mass derived from $L_{H\beta}$. In the next analysis, we just consider the mass and Eddington ratio calculated from $\lambda L_{\lambda}(5100\text{\AA})$.

In the top panel of Figure 4, we plot the deviation of the SMBH mass from $M_{\text{BH}} - \sigma_*$ relation versus the radio loudness. It is obvious that the deviation tends to be larger when radio loudness becomes larger. In the bottom panel of Figure 4, we also plot the deviation of the SMBH mass from the $M_{\text{BH}} - \sigma_*$ relation versus the redshift. We find a weak correlation between the mass deviation and the redshift for radio-quiet quasars. The simple least-square regression gives: $\Delta \log M_{\text{BH}} = (1.00 \pm 0.06)z - (0.29 \pm 0.03)$. The correlation coefficient R is 0.26, with a probability of $p_{\text{null}} < 10^{-4}$ for rejecting the null hypothesis of no correlation. In

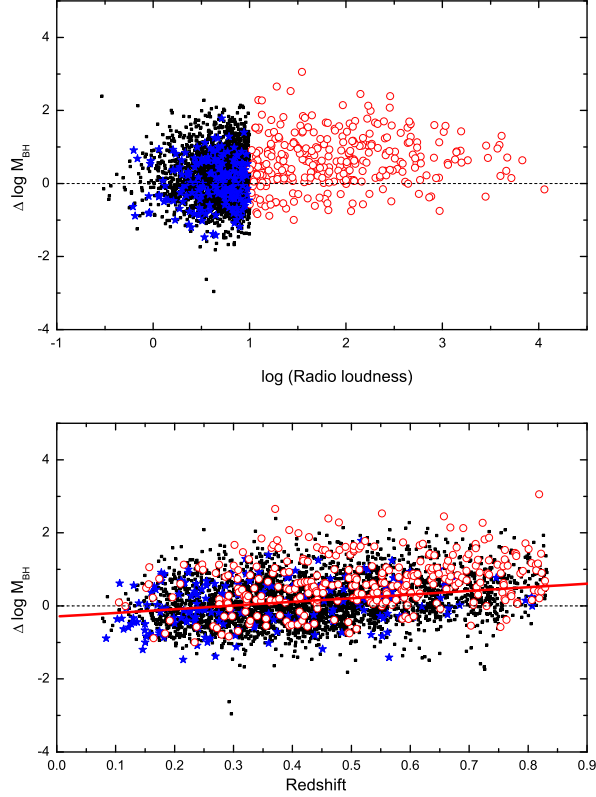


Fig. 4 Top: The deviation of the SMBH mass from the Tremaine’s $M_{\text{BH}} - \sigma_*$ relation in fig 2. versus the radio loudness. The dash line denotes $\Delta \log M_{\text{BH}} = 0$. Bottom: The deviation of the SMBH mass from the Tremaine’s $M_{\text{BH}} - \sigma_*$ relation in fig 2. versus the redshift. The red solid line denotes our best fit for all radio-quiet quasars. Symbols as Figure 3.

Figure 5, we show the redshift distributions for radio-quiet and radio-loud quasars. The radio-loud quasars (red circles) have larger redshifts relative to the radio-quiet quasars (blue stars) (see Figure 5).

In Table 1, we show the mean values of the masses and the Eddington ratios in different redshift bins for different samples.

4.2 Uncertainties

There are some factors to account for the uncertainty of the SMBH mass calculation: the uncertainties of $H\beta$, $[O \text{ III}]$ line widths, $\lambda L_\lambda(5100\text{\AA})$, $L_{H\beta}$ when the multi-components are used to model SDSS spectra; the system errors in equations (1-5) from the uncertainties of the BLRs geometry and dynamics. The uncertainty of our calculated SMBH mass is about 0.5 dex. The uncertainty of the Eddington ratio is about 0.5 dex or more. For radio-loud quasars, we should account two effect: the relativistic beaming effect on the optical continuum and the orientation of BLRs. The total $H\beta$ luminosity instead of $\lambda L_\lambda(5100\text{\AA})$ is used to account for the first effect. We find the effect is small in our sample, and there is no correlation between the $H\beta$ EW and the radio loudness (e.g. Wu et al. 2004). Lacy et al. (2001) made a small correction of the orientation of BLRs by a factor of $R_c^{0.1}$, where R_c is the ratio of core to extended radio luminosity.

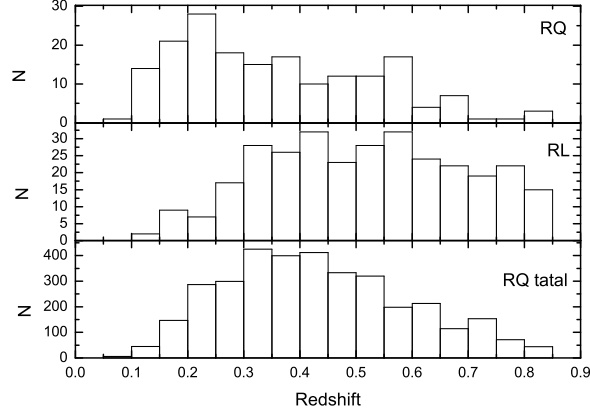


Fig. 5 The redshift distributions for 181 radio-quiet quasars with radio loudness (top), 306 radio-loud quasars with measured radio luminosity (middle), total 3466 radio-quiet quasars (bottom).

They adopted $R_c = 0.1$ for steep-spectrum quasars and $R_c = 10$ for flat-spectrum quasars if R_c is not measured. It will lead to the uncertainties of $\Delta \log M_{\text{BH}}$ about 0.2 dex.

The fibers in the SDSS spectroscopic survey have a diameter of $3''$ on the sky. The SDSS spectra of lower-redshift quasars possibly have obvious stellar light contribution, which can be used to directly measure the stellar velocity dispersion (e.g., Kauffmann et al. 2003; Heckman et al. 2004; Bian et al. 2006). For luminous quasars ($M_i < -22$), the stellar light contribution can be omitted or has little effect on the mass calculation (e.g., Vanden Berk et al. 2006).

It is possible that jet can have a dynamical effect on the NLRs and may have a systematically different effect on the [O III] profile (Nelson & Whittle 1996). However, considering the [O III] profile broadening by jet, the correction of [O III] gas velocity dispersion will lead the radio-loud quasars to deviate much more from the $M_{\text{BH}} - \sigma_*$ relation.

We select quasars with the EW of narrow [O III] component larger than 1.5, EW errors of H β and [O III] $\lambda\lambda 4959, 5007$ less than 100%. Different criteria would lead to different number of quasars (such as error of EWs less than 5%, 50%, or 100%, $\chi^2 < 4$). However, we find that the main results don't change. In the next subsection, we will discuss the luminosity bias in detail.

4.3 The mass deviation from the luminosity bias

Salviander et al. (2007) also used SDSS DR3 quasars to discuss the cosmological evolution of $M_{\text{BH}} - \sigma_*$ relation. After carefully consider the selection biases and intrinsic scatter in the $M_{\text{BH}} - \sigma_*$ relation, they suggested that $M_{\text{BH}} - \sigma_*$ relation appears to evolve with redshift. Netzer & Trakhtenbrot (2007) also found the nonlinear $M_{\text{BH}} - \sigma_*$ relation with the different slopes for different redshift bins. During our process of selecting objects, the line fitting favor the brighter objects (i.e. luminosity bias, see Figure 6). Following the work of Salviander et al. (2007), we calculate the contribution of $\Delta \log M_{\text{BH}}$ from this luminosity bias. We calculate the mean observed luminosity in different redshift bins for our different samples (i.e. RQ total sample; RQ sample; RL sample). Using the QSOs luminosity function (Boyle et al., 2000), we calculate the cut luminosity to make the mean luminosity of the kept QSOs ($L > L_{\text{cut}}$) equal to the observed mean luminosity in different redshift bin. Then we do the simulation to calculate the contribution of $\Delta \log M_{\text{BH}}$ from this luminosity bias (for detail in Salviander et al. 2007). We obtained a formulae: $\Delta \log M_{\text{BH}}^{\text{simu}} = 0.292 + 0.1138x + 0.265x^2 + 0.480x^3 + 0.182x^4$, where x is $\log(L_{\text{cut}}/L_0)$, $L_0 = 0.3L_{\text{Edd}}(M_{\text{gal}}^*)$, $M_{\text{gal}}^* = 10^{11}M_{\odot}$ (Drory et al. 2005). We find that the mass deviation form the

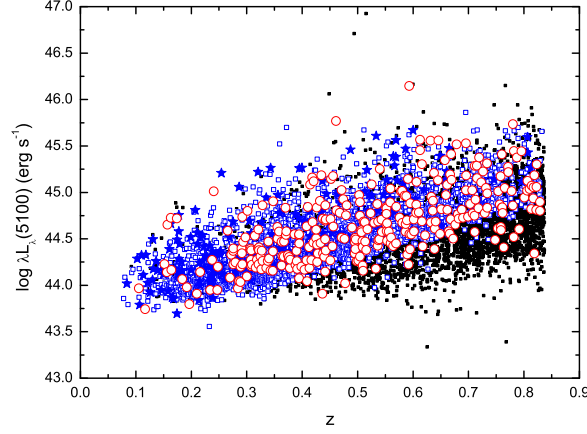


Fig. 6 $\lambda L_{\lambda}(5100\text{\AA})$ versus z . Open circles denote RL sample; blue stars denote RQ QSOs with measured radio loudness; blue squares denote RQ QSOs with upper-limits of radio loudness; small black squares denote all 9753 SDSS DR3 QSOs with $z < 0.83$. It is obvious that some faint objects are missed in our selection.

z (1)	N (2)	$\log(\lambda L_{\lambda}(5100\text{\AA}) \text{ erg s}^{-1})$ (3)	$\log(M_{\text{BH}}/M_{\odot})$ (4)	$\log(L_{\text{Bol}}/L_{\text{Edd}})$ (5)	$\Delta \log M_{\text{BH}}$ (6)	$\log L_{\text{cut}}/L_0$ (7)	$\Delta \log M_{\text{BH}}^{\text{simu}}$ (8)
RQ Total							
0.1-0.2	198	44.08 ± 0.17	7.81 ± 0.41	-1.05 ± 0.40	-0.08 ± 0.54	-1.38	0.04
0.2-0.3	586	44.17 ± 0.21	7.92 ± 0.39	-1.06 ± 0.37	-0.02 ± 0.61	-1.30	0.06
0.3-0.4	824	44.32 ± 0.24	8.05 ± 0.43	-1.02 ± 0.36	0.07 ± 0.58	-1.18	0.09
0.4-0.5	745	44.48 ± 0.22	8.24 ± 0.41	-0.98 ± 0.36	0.08 ± 0.61	-0.98	0.15
0.5-0.6	518	44.67 ± 0.24	8.49 ± 0.43	-0.97 ± 0.37	0.30 ± 0.61	-0.74	0.21
0.6-0.7	327	44.82 ± 0.23	8.62 ± 0.43	-0.93 ± 0.33	0.37 ± 0.60	-0.58	0.24
0.7-0.83	267	45.04 ± 0.23	8.80 ± 0.39	-0.87 ± 0.34	0.41 ± 0.63	-0.38	0.26
RQ							
0.1-0.4	114	44.35 ± 0.32	8.21 ± 0.32	-1.01 ± 0.39	-0.04 ± 0.63	-1.14	0.10
0.4-0.82	67	44.94 ± 0.34	8.62 ± 0.41	-0.83 ± 0.32	0.17 ± 0.61	-0.50	0.25
RL							
0.1-0.3	35	44.25 ± 0.29	8.25 ± 0.38	-1.15 ± 0.42	0.01 ± 0.68	-1.22	0.08
0.3-0.5	109	44.49 ± 0.31	8.51 ± 0.45	-1.17 ± 0.39	0.52 ± 0.80	-0.98	0.15
0.5-0.7	106	44.78 ± 0.35	8.78 ± 0.38	-1.14 ± 0.32	0.80 ± 0.63	-0.66	0.23
0.7-0.83	56	44.98 ± 0.29	8.91 ± 0.39	-1.08 ± 0.33	0.95 ± 0.75	-0.46	0.26

Table 1 The mean quantities in different redshift bins for different samples. L_{cut} is calculated from the QSOs luminosity function (Boyle et al. 2000) to make the mean luminosity of the kept QSOs ($L > L_{\text{cut}}$) equal to the observed mean luminosity in different redshift bins. $L_0 = 0.3L_{\text{Edd}}(M_{\text{gal}}^*)$, where $M_{\text{gal}}^* = 10^{11}M_{\odot}$ in the galaxy mass function $\Phi(M_{\text{gal}}) = \Phi^*(M_{\text{gal}}/M_{\text{gal}}^*)^{-a}e^{-M_{\text{gal}}/M_{\text{gal}}^*}$ (Drory et al. 2005).

luminosity bias is monotonously increased with the redshift (see Col.(8) in Table 2). Table 1 shows our results. Col.(1) is the redshift bin; Col.(2) is the number in the redshift bin; Col.(3)-(5) are the mean values of 5100 Å luminosity, mass, Eddington ratio; Col.(6) is the mean mass deviation from $M_{\text{BH}} - \sigma_*$ relation; Col.(7) is $\log(L_{\text{cut}}/L_0)$; Col.(8) is our simulated mass deviation for different cut luminosity in different redshift bins.

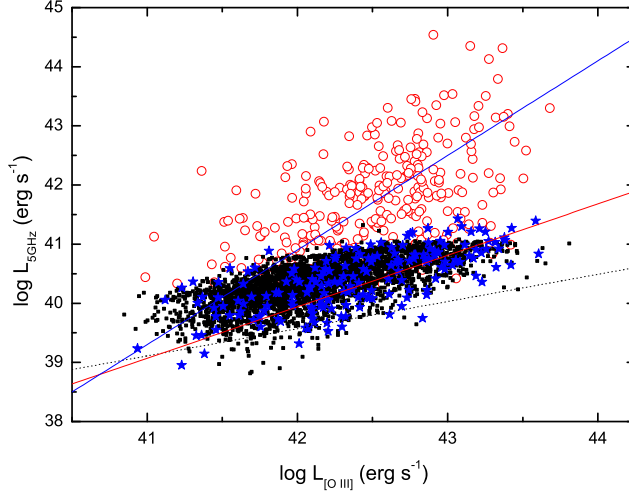


Fig. 7 The radio luminosity versus the [O III] luminosity. Red circle denotes radio-loud quasars, blue star denotes radio-quiet quasars with measured radio luminosity, black square denotes the radio-quiet quasars with upper-limit of the radio luminosity. The red solid line is the BCES bisector result for radio-quiet quasars (blue stars). The blue solid line is the BCES bisector result for radio-loud quasars (red circles). The dash line is the best fit of radio-quiet AGNs found by Xu et al. (1999).

For RQ total sample, the luminosity bias can interpret most amount of $\Delta \log M_{\text{BH}}$. For the highest redshift bin of $0.7 < z < 0.83$, $\Delta \log M_{\text{BH}}$ is about 0.15 dex after correction the effect of luminosity bias. This 0.15 dex is possibly the $M_{\text{BH}} - \sigma_*$ cosmological evolution in this highest redshift bin, which is very consistent with the result of Salvander et al. (2007). However, we should note that the standard deviation of $\Delta \log M_{\text{BH}}$ in different bins is about 0.6dex, which is very larger than this 0.15dex. For RQ sample, the observed $\Delta \log M_{\text{BH}}$ can be completed contributed from the luminosity bias, which is possibly due to the smaller numbers of this sample. Therefore, we think there is no obvious deviation from $M_{\text{BH}} - \sigma_*$ relation considering the M_{BH} uncertainties and the luminosity bias.

For RL sample, after corrected the contribution from the luminosity bias, $\Delta \log M_{\text{BH}}$ is still large (about 0.69 dex in $0.7 < z < 0.83$) and there is a trend that $\Delta \log M_{\text{BH}}$ becomes larger for larger redshift bin. Considering the possible $M_{\text{BH}} - \sigma_*$ cosmological evolution (0.15 dex in $0.7 < z < 0.83$), for radio loud QSOs, there are still 0.54 dex deviation in $0.7 < z < 0.83$. Bonning et al. (2005) suggested that narrower [O III] for radio loud quasars is responsible for this deviation from the $M_{\text{BH}} - \sigma_*$ relationship, and it is not the effect involving M_{BH} . The cause of this deviation is unclear.

5 ORIGIN OF RADIO LUMINOSITY

5.1 $L_{5\text{GHz}} - L_{[\text{O III}]}$ relation

The relation between the radio luminosity and the optical/X-ray luminosity, which provides the connection between the jet and accretion power, have been discussed by many group (e.g. Xu et al. 1999; Ho 2002; Wang et al. 2004; Panessa et al. 2007; Sikora 2007). In Figure 7, we show the radio luminosity at 5GHz versus the total [O III] luminosity. These two luminosities are all related to the redshift. By the partial Kendall's τ correlation test, we do a partial correlation analysis with redshift as the test variable (Akritas

& Siebert 1996). For the RQ sample of 181 radio-quiet quasars, partial Kendall's τ correlation is 0.237, variance is 0.0304, and the probability of null hypothesis is 6.3×10^{-15} . For RL sample of 306 radio-loud quasars, τ correlation is 0.251, variance is 0.0456, and the probability of null hypothesis is 3.7×10^{-8} . We use the bivariate correlated errors and intrinsic scatter (BCES) regression method¹ of Akritas & Bershady (1996) (see also Isobe et al. 1990) to find the relation between $L_{[\text{O III}]}$ and $L_{5\text{GHz}}$, and adopt the BCES bisector result (e.g. Kaspi et al. 2005). For RQ sample of 181 radio-quiet quasars with measured radio luminosity, the BCES bisector result: $\log L_{5\text{GHz}} = (0.87 \pm 0.04)\log L_{[\text{O III}]} + (3.40 \pm 1.87)$ (red dash line in Figure 7). For RL sample of 306 radio-loud quasars, $\log L_{5\text{GHz}} = (1.60 \pm 0.08)\log L_{[\text{O III}]} - (26.30 \pm 3.39)$.

In Figure 7, considering the errors of the intercept, our best fits for radio-quiet quasars is consistent with the result found by Xu et al. (1999) (also see Ho & Peng 2001): $\log L_{5\text{GHz}} = (0.45 \pm 0.07)\log L_{[\text{O III}]} + (20.25 \pm 0.6)$ (black dot line in Figure 7). In the plot of radio luminosity versus the optical/X-ray nuclear luminosity, the separation of radio-loud and radio-quiet quasars from SDSS DR3 is not too clear as other's results (Xu et al. 1999; Terashima & Wilson 2003; Sikora et al. 2007). The difference is possibly due to the selection effect by different wavelength bands.

[O III] luminosity is usually assumed to be proportional to the accretion rate and this correlation can be explained in a model of accelerated and collimated jet by magnetic field (Xu et al. 1999). Apart from the dependence on the accretion rate, the radio luminosity possibly depends on the central SMBH properties, mass or spin (e.g., Sokira et al. 2007 and refs. therein), which we will discuss in the next section.

If we use the tight correlation between X-ray luminosity and [O III] luminosity (e.g., Xu et al. 1999), $\log L_x = 1.01\log L_{[\text{O III}]} + 1.6$, the relation between $L_{5\text{GHz}}$ and $L_{[\text{O III}]}$ can be transformed to the relation between $L_{5\text{GHz}}$ and L_x : $L_{5\text{GHz}} \propto L_x^{0.86 \pm 0.06}$ for RQ sample and $L_{5\text{GHz}} \propto L_x^{1.58 \pm 0.10}$ for RL sample. There exists obvious different on the slope for radio-quiet and radio-loud quasars. For low luminosity AGNs, Panessa et al. (2007) suggested a correlation, $L_x \propto L_{5\text{GHz}}^{0.97}$, their index is between ours for radio-quiet and radio-loud quasars. If we use the correlation suggested by Netzer et al. (2006), $L_{\text{O III}} \propto L_x^{0.704 \pm 0.06}$, the relation we found between $L_{5\text{GHz}}$ and $L_{[\text{O III}]}$ can be transformed to $L_{5\text{GHz}} \propto L_x^{0.61 \pm 0.04}$ for RQ sample and $L_{5\text{GHz}} \propto L_x^{1.11 \pm 0.07}$ for RL sample. The radio luminosity is often assumed coming from the relativistic electrons powered by a jet. The result of RL sample is consistent with that of Panessa et al. (2007). The X-ray emission is often assumed coming from both the accretion flow and the relativistic jet, dominated by accretion flow at high accretion rate, and dominated by jet emission at low accretion rate. (Gallo et al. 2003; Yuan & Cui 2005). This relation between $L_{5\text{GHz}}$ and L_x in different accretion rates can be explained in the jet-dominant X-ray models (e.g., Fender et al. 2003; Gallo et al. 2003; Heinz 2004; Yuan & Cui 2005).

5.2 The radio luminosity dependence on the SMBH mass and the Eddington ratio

It is suggested that the radio luminosity/radio loudness is relate to the SMBH masses (e.g., Laor 2000). We calculate the radio luminosity dependence on the SMBH mass and the Eddington ratio, i.e. $\log L_{5\text{GHz}} = a + b_1 \log M_{\text{BH}} + b_2 \log(L_{\text{Bol}}/L_{\text{Edd}})$ (see Figure 8).

We firstly do the multiple regression with ASURV Rev 1.2 (LaValley, Isobe & Feigelson 1992 and refs. therein) for RQ sample, RL sample and RL+RQ sample. In order to avoid the non-symmetric regression, a, b_1, b_2 are adopted the mean values when we use different variable as the dependent variables in the multiple regressions (see Col.(1) in Table 1). In all the multiple regressions, the probability for rejecting the null hypothesis of no correlation is $p_{\text{null}} < 10^{-4}$. The R-Square correlation coefficient for RQ sample is larger than other two samples (see Table 2, Figure 8).

We also do the symmetric multivariate regression analysis, through the equation $y = a + b_1 x_1 + b_2 x_2$, directly by the χ^2 estimator, $\chi^2 = \sum_i \frac{(y_i - a - b_1 x_{1i} + b_2 x_{2i})^2}{\sigma_{y_i}^2 + (b_1 \sigma_{x_{1i}})^2 + (b_2 \sigma_{x_{2i}})^2}$, (Press et al. 1992; Tremaine et al., 2002; Merloni et al., 2003), where σ are the corresponding uncertainties. Considering the same uncertainties (σ) of radio luminosity, mass, and the Eddington ratio (Tremaine et al., 2002; Merloni et al., 2003), we re-normalized these uncertainties to make the minimum χ^2/n_{dof} of unity, the results are listed in first lines for different sample in Table 1.

Considering the errors of a, b_1, b_2 in Tables 2, the results from ASURV and χ^2 are consistent very well. Therefore, in the next analysis, we adopt the values of a, b_1, b_2 from χ^2 estimator (Table 1), i.e. $L_{5\text{GHz}} \propto$

¹ This is not a symmetric regression used by Merloni et al. 2003. For detail in section 5.2

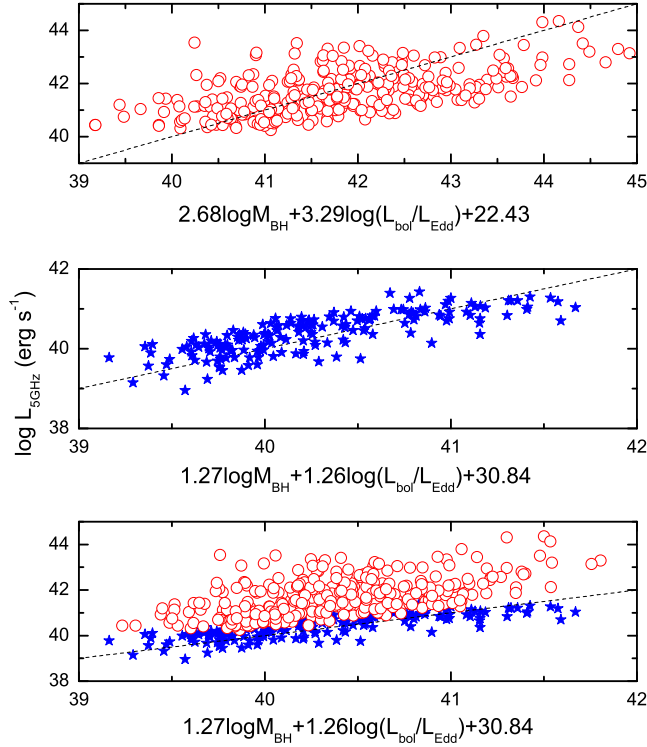


Fig. 8 The radio luminosity dependence on the SMBH mass and the Eddington ratio. The indexes are adopted from the mean values in brackets in Table 1. Top panel is for radio-loud quasars, middle panel is for radio-quiet quasars with measured radio luminosity, bottom panel is for them all. Symbols as Figure 7. The dash lines denote 1:1.

$M_{\text{BH}}^{1.28^{+0.23}_{-0.16}} (L_{\text{Bol}}/L_{\text{Edd}})^{1.29^{+0.31}_{-0.24}}$ for RQ sample, and $L_{5\text{GHz}} \propto M_{\text{BH}}^{3.10^{+0.60}_{-0.70}} (L_{\text{Bol}}/L_{\text{Edd}})^{4.18^{+1.40}_{-1.10}}$ for RL sample, and $L_{5\text{GHz}} \propto M_{\text{BH}}^{4.30^{+0.70}_{-0.80}} (L_{\text{Bol}}/L_{\text{Edd}})^{5.15^{+2.32}_{-1.69}}$ for RL+RQ sample.

Ho (2002) suggested a correlation between the nuclei radio loudness and the Eddington ratio (Gallo et al. 2003; Greene et al. 2006; Sikora et al. 2007; Panessa et al. 2007). We also use the multiple regression by ASURV to search the radio loudness dependence on the SMBH mass and the Eddington ratio (set radio luminosity as the dependent variable). However, the R-Square correlation coefficient is very low for RL sample and RQ sample. For the RL+RQ sample, we find a weak correlation between the radio loudness and the SMBH mass (the simple least-square correlation $R=0.26$), much weaker correlation between the radio loudness and the Eddington ratio ($R=-0.15$). The range of Eddington ratio is between 0.01 to 1 for our RL sample and RQ sample. And our sample is composed by broad line type I quasars, which just fill the gaps between two sequences in plot of radio loudness versus the Eddington ratio (see Figure 3 in Sikora et al. 2007). When we research the disk-jet connection model, X-ray luminosity is maybe a better tracer of SMBHs accretion power than the optical luminosity (e.g. Panessa et al. 2007). We also should pay more attention on narrow-line Seyfert 1 galaxies with larger Eddington ratios in this kind of plot (e.g. Zhou & Wang 2002; Whalen et al. 2006; Komossa et al. 2006).

Table 2 The mean quantities in different redshift bins for different samples. a, b_1, b_2 is defined by: $\log L_{5\text{GHz}} = a + b_1 \log M_{\text{BH}} + b_2 \log(L_{\text{Bol}}/L_{\text{Edd}})$. For different samples, the first line is for the result by χ^2 minimization, and in the second line, quantities in brackets are the mean values of a, b_1, b_2 by ASURV, the last three lines are results considering different dependent variable by ASURV.

Dependent variable (1)	a (2)	b_1 (3)	b_2 (4)	R-sqaure (5)
RQ	$30.9^{+1.20}_{-1.80}$ (30.84 ± 2.21)	$1.28^{+0.23}_{-0.16}$ (1.27 ± 0.29)	$1.29^{+0.31}_{-0.24}$ (1.26 ± 0.53)	
$L_{5\text{GHz}}$	33.18 ± 0.43	0.95 ± 0.05	0.81 ± 0.07	0.64
M_{BH}	28.79 ± 1.54	1.52 ± 0.02	1.12 ± 0.08	0.72
$L_{\text{Bol}}/L_{\text{Edd}}$	30.54 ± 3.04	1.35 ± 0.09	1.85 ± 0.02	0.57
RL	$19.7^{+5.40}_{-3.90}$ (22.43 ± 10.4)	$3.10^{+0.60}_{-0.70}$ (2.68 ± 1.30)	$4.18^{+1.40}_{-1.10}$ (3.29 ± 1.94)	
$L_{5\text{GHz}}$	32.62 ± 0.82	1.24 ± 0.10	1.38 ± 0.13	0.35
M_{BH}	11.77 ± 3.54	3.85 ± 0.40	3.23 ± 0.19	0.53
$L_{\text{Bol}}/L_{\text{Edd}}$	22.89 ± 3.79	2.95 ± 0.16	5.26 ± 0.05	0.49
RL+RQ	$10.0^{+8.70}_{-4.20}$ (15.65 ± 12.93)	$4.30^{+0.70}_{-0.80}$ (3.46 ± 1.81)	$5.15^{+2.32}_{-1.69}$ (4.11 ± 3.81)	
$L_{5\text{GHz}}$	30.45 ± 0.73	1.38 ± 0.09	0.92 ± 0.12	0.31
M_{BH}	6.57 ± 2.74	4.34 ± 0.04	3.09 ± 0.17	0.53
$L_{\text{Bol}}/L_{\text{Edd}}$	9.92 ± 4.67	4.67 ± 0.25	8.33 ± 0.08	0.40

For scale-free jet physics, Heinz & Sunyaev (2003) derived the dependence of the accretion-powered jets flux (f_v) upon the SMBH mass and the dimensionless accretion rates for different accretion scenarios (see their Table 1). For radiation-pressure-supported standard accretion disk, $f_v \propto M_{\text{BH}}^{17/12-\alpha/3}$; for gas-pressure-supported standard accretion disk, $f_v \propto M_{\text{BH}}^{(187-32\alpha)/120} \dot{m}^{(17/12+2\alpha/3)4/5}$; for ADAF, $f_v \propto M_{\text{BH}}^{17/12-\alpha/3} \dot{m}^{17/12+2\alpha/3}$, where α is the radio spectral index. Assuming $\alpha = 0.5$, for radiation-pressure-supported standard accretion disk, $f_v \propto M_{\text{BH}}^{1.25}$; for gas-pressure-supported standard accretion disk, $f_v \propto M_{\text{BH}}^{1.43} \dot{m}^{1.40}$; for ADAF, $f_v \propto M_{\text{BH}}^{1.25} \dot{m}^{1.75}$. Considering large scatter in b_1, b_2 , our results are consistent with above the radio origin of scale-free jet model. However, by our data, we can't distinguish the different disks for radio-quiet and radio-loud quasars in this accretion-powered jet model.

6 CONCLUSIONS

With the large number of quasars in SDSS DR3 catalog, we use the multi-components to model the SDSS spectra and calculate the SMBH masses. Combined with the radio properties from FIRST, we obtained a sample of 3772 quasars with reliable SMBH masses, including 306 radio-loud quasars, 3466 radio-quiet quasars with measured radio luminosity or upper-limit of radio luminosity (181 radio-quiet quasars with measured radio luminosity). Two main results are suggested: (1) The radio-loud quasars deviate much from the $M_{\text{BH}} - \sigma_*$ relation of the nearby normal galaxies defined by Tremaine et al. (2002) respect to that for radio-quiet quasars, which is only partly due to the possible cosmology evolution of the $M_{\text{BH}} - \sigma_*$ relation and the luminosity bias. (2) The radio luminosity is correlated to the central SMBH mass and the Eddington ratio, $\propto M_{\text{BH}}^{1.28^{+0.23}_{-0.16}} (L_{\text{Bol}}/L_{\text{Edd}})^{1.29^{+0.31}_{-0.24}}$ for radio-quiet quasars and $\propto M_{\text{BH}}^{3.10^{+0.60}_{-0.70}} (L_{\text{Bol}}/L_{\text{Edd}})^{4.18^{+1.40}_{-1.10}}$ for radio-loud quasars. Weaker correlation coefficient of the radio luminosity dependence upon the mass and the Eddington ratio for radio-loud quasars shows other physical effects would account for their radio luminosity, such as the SMBH spin.

ACKNOWLEDGMENTS

We thank Luis C. Ho for his very helpful comments. We thank Dr. M. Wu and Z. H. Fan for the discussion. We thank the anonymous referee for his/her comments and instructive suggestions. This work has been supported by the NSFC (Nos. 10733010, 10403005, 10325313, 10233030 and 10521001), the Science-Technology Key Foundation from Education Department of P. R. China (No. 206053), and China

Postdoctoral Science Foundation (No. 20060400502). Chen Hu thanks T. A. Boroson & M. Vestergaard for the I ZW 1 iron templates and their so kindly suggestions on the spectral fitting.

Funding for the creation and distribution of the SDSS Archive has been provided by the Alfred P. Sloan Foundation, the Participating Institutions, the National Aeronautics and Space Administration, the National Science Foundation, the US Department of Energy, the Japanese Monbukagakusho, and the Max Planck Society. The SDSSWeb site is <http://www.sdss.org>. The SDSS is managed by the Astrophysical Research Consortium for the Participating Institutions. The Participating Institutions are the University of Chicago, Fermilab, the Institute for Advanced Study, the Japan Participation Group, The Johns Hopkins University, the Korean Scientist Group, Los Alamos National Laboratory, the Max Planck Institute for Astronomy, the Max Planck Institute for Astrophysics, New Mexico State University, the University of Pittsburgh, the University of Portsmouth, Princeton University, the United States Naval Observatory, and the University of Washington.

This research has made use of the NED database, which is operated by the Jet Propulsion Laboratory, California Institute of Technology, under contract with the National Aeronautics and Space Administration.

References

- Abazajian K., et al., 2005, *AJ*, 129, 1755
Akritas M. G., Bershadsky M. A., 1996, *ApJ*, 470, 706
Akritas M. G., Siebert J., 1996, *MNRAS*, 278, 919
Begelman M. C., Blandford R. D., Rees M. J., 1984, *Rev. Mod. Phys.*, 56, 255
Bian W., Zhao Y., 2004, *MNRAS*, 347, 607
Bian W., Gu Q., Zhao Y., Chao L., Cui Q., 2006, *MNRAS*, 372, 876
Blundell K. M., Beasley A. J., 1998, *MNRAS*, 299, 165
Bonning E. W., Shields G. A., Salviander S., McLure R. J., 2005, *ApJ*, 626, 89
Boroson T. A., 2003, *ApJ*, 585, 647
Boroson T. A., Green R. F., 1992, *ApJS*, 80, 109
Boyle B. J., Shanks T., Croom S. M., Smith R. J., Miller L., Loaring N., Heymans C., 2000, *MNRAS*, 317, 1014
Cardelli J. A., Clayton G. C., Mathis J. S., 1989, *ApJ*, 345, 245
Collin S. et al., 2006, *A&A*, 456, 75
Dasyra K. M., et al., 2007, *ApJ*, 657, 102
Drory N., Salvato M., Gabasch A., Bender R., Hopp U., Feulner G., Pannella M., 2005, *ApJ*, 619, L131
Ferrarese L., Merritt D., 2000, *ApJ*, 539, L9
Franceschini A., Vercellone S., Fabian A. C., 1998, *MNRAS*, 297, 817
Fender R. P., Gallo E., Jonker P. G., 2003, *MNRAS*, 343, L99
Gallo E., Fender R. P., Pooley G. G., 2003, *MNRAS*, 344, 60
Gebhardt K., et al., 2000, *ApJ*, 539, L13
Grandi S. A., 1982, *ApJ*, 255, 25
Greene J. E., Ho L. C., 2005a, *ApJ*, 627, 721
Greene J. E., Ho L. C., 2005b, *ApJ*, 630, 122
Greene J. E., Ho L. C., Ulvestad J. S., 2006, *ApJ*, 636, 56
Greene J. E., Ho L. C., 2006, *ApJ*, 641, L21
Grupe D., Mathur S., 2004, *ApJ*, 606, L41
Heinz S., 2004, *MNRAS*, 355, 835
Heinz S., Sunyaev R. A., 2003, *MNRAS*, 343, L59
Heckman T. M., et al., 2004, *ApJ*, 613, 109
Ho L. C., 2002, *ApJ*, 564, 120
Ho L. C., Peng C. Y., 2001, *ApJ*, 555, 650

- Isobe T., et al., 1990, ApJ, 364, 104
- Kaspi S., Maoz D., Netzer H., Peterson B.M., Vestergaard M., Jannuzi B.T., 2005, ApJ, 629, 61
- Kaspi S., Smith P.S., Netzer H., Maoz D., Jannuzi B.T., Giveon U., 2000, ApJ, 533, 631
- Kauffmann G., et al., 2003, MNRAS, 346, 1055
- Kellermann K.I., Sramek R., Schmidt M., et al., 1989, AJ, 98, 1195
- Komossa S., Voges W., Xu D., et al., 2006, AJ, 132, 531
- Komossa S., Xu D., 2007, 667, L33
- Lacy M., et al., 2001, ApJ, 551, L17
- Laor A., 2000, ApJ, 543, L111
- Laor A., 2003, astro-ph/0312417
- Lauer T. R., et al., 2007, ApJ, 622, 808
- LaValley M.P., Isobe T., Feigelson E.D., 1992, BAAS, 24, 839
- Liu Y., Jiang D. R., Gu M. F., 2006, ApJ, 637, 669
- McLure R. J., Jarvis M. J., 2004, MNRAS, 353, L45
- Merloni A., Heinz S., Di Matteo T., 2003, MNRAS, 345, 1057
- Merloni A., et al., 2006, New Astr. 11, 567
- Nelson C. H., 2001, ApJ, 544, L91
- Nelson C. H., Whittle M., 1996, ApJ, 465, 96
- Netzer H. et al., 2006, A&A, 453, 525
- Netzer H., Trakhtenbrot B., 2007, ApJ, 654, 754
- O'Donnell James E., 1994, ApJ, 422, 158
- Onken C. A., et al., 2004, ApJ, 615, 645
- Peterson B. M., et al., 2004, ApJ, 613, 682
- Panessa et al., 2007, A&A, astro-ph/0701546
- Richards G. T., et al., 2006, ApJS, 166, 470
- Sandage A., 1965, ApJ, 141, 1560
- Salviander S., et al., 2007, ApJ, 622, 131
- Schneider D. P. et al., 2005, AJ, 130, 367
- Shen J.-J., et al., 2008, AJ, 135, 928
- Shields J. C., et al., 2003, ApJ, 583, 124
- Sikora M., Stawarz L., Lasota J., 2007, ApJ, 658, 851
- Storey P. J., Hummer D. G., 1995, MNRAS, 272, 41
- Strittmatter P.A., Hill P., Pauliny-Toth I.I.K., et al., 1980, A&A, 1980, 88, L12
- Sulentic J.W., Marziani P., Dultzin-Hacyan D., 2000, ARA&A, 38, 521
- Terashima Y, Wilson A.S., 2003, ApJ, 583, 145
- Treu T., Malkan M. A., Blandford R. D., 2004, ApJ, 615, L97
- Tremaine S., et al., 2002, Ap J, 574, 740
- Vanden Berk, et al., 2006, AJ, 131, 84
- Whalen D.J., Laurent-Muehleisen S.A., Moran E.C., Becker R.H., 2006, AJ, 131, 1948
- Wang J. M., Luo B., Ho L. C., 2004, ApJ, 615, L9
- Wang R, Wu X.B., Kong M. Z., 2006, ApJ, 645, 890
- Wills B.J., Browne I.W.A., 1986, ApJ, 302, 56
- Woo J. H., Urry C. M., 2002, ApJ, 581, L5
- Woo J. H., et al., 2006, ApJ, 645, 900
- Xu C., Livio M., Baum S. A., 1999, AJ, 118, 1169
- Wu X.-B., Wang R., Kong M. Z., Liu F. K., Han J. L., 2004, A&A, 424, 793

Yuan F., Cui W., 2005, ApJ, 629, 408
Zhou H. Y., et al., 2006, ApJS, 166, 128
Zhou H., Wang T., 2002, ChJAA, 2, 501